

11.3 ACTIVE TURBULENCE OVER AN OUTDOOR REDUCED URBAN SCALE MODEL

Atsushi Inagaki* and Manabu Kanda*
 * Tokyo Institute of Technology, Tokyo, Japan

1. INTRODUCTION

Townsend (1976) hypothesized that the turbulent boundary layer is composed of active and inactive motions. The active motion directly contributes to the Reynolds stress and inactive motion does not contribute to it. Inagaki and Kanda (2008) observed that both kinds of motion exist within the atmospheric surface layer over building-like roughness. Therefore, turbulent transport process of momentum, heat and scalars in the surface layer is expected to relate to the active motion. However, it is difficult to investigate the characteristics of active motion itself because the active and inactive motions always coexist.

Inagaki and Kanda (2010) proposed a method to separate the active and inactive motion in the instantaneous turbulent flow, and validated this method using the datasets obtained in the comprehensive outdoor scale model experiment for urban climate (COSMO). In this report, we used this separation method and examined the statistical and structural characteristics of the active motion developed over the COSMO experimental facility.

2. METHOD TO SEPARATE THE ACTIVE AND INACTIVE MOTIONS

Inagaki and Kanda (2010) proposed a method to separate the active and inactive turbulence for understanding the nature of active motion. The method is based on the assumption that the active and inactive turbulence do not directly interact with each other because the size of the inactive motion is much larger than that of the active motion (Townsend, 1976). Then, the active and inactive turbulence can be linearly separated. The validity of this separation has been discussed by McNaughton & Laubach (1998) and Inagaki & Kanda (2008).

In conventional experimental studies of turbulence, turbulence component is usually defined as the residuals from the temporal average if the data are based on a single point measurement,

$$\varphi = \bar{\varphi} + \varphi', \quad (1)$$

where φ is a physical variable, such as the velocity component or temperature. The over bar and the prime indicate the temporal mean and fluctuation

* Corresponding author address: Atsushi Inagaki, Tokyo Institute of Technology, Dept. of International Development Engineering, Meguro-ku, O-okayama, 2-12-1 I4-9 Tokyo, 152-8552 JAPAN; e-mail: inagaki.a.ab@m.titech.ac.jp

terms, respectively. Hereafter, this conventional definition of fluctuation is called 'TD'. TD generally involves both active and inactive fluctuation components if the averaging time is larger than the time scale of the inactive motion.

To separate the contribution of the low-frequency inactive motion, we used an instantaneous line average along the spanwise direction,

$$\varphi = [\varphi]_m + \bar{\varphi}'_m + \varphi'', \quad (2)$$

where the square brackets and prime with subscript m indicate the mean part of the line average and residual fluctuation part, respectively. If the area for the line average is sufficiently larger than the size of the active turbulence and sufficiently smaller than the size of the inactive motions, then the inactive motions can be approximated by the mean part of Eq. (2). The fluctuation defined in Eq.2 is called 'SD'.

3. EXPERIMENT

3.1 COSMO

The COSMO experimental facility was constructed at the Nippon Institute of Technology in Saitama, Japan. There are 512 concrete cubes and 8-meter meteorological towers on a flat concrete plate (Figure 1). The cubes, which are 1.5 m (=H) on a side, are arranged regularly. Detailed descriptions of COSMO can be found in Kanda et al. (2007) and Inagaki & Kanda (2008). The mean wind direction was usually from the northwest during the experiments in this study.

The mean flow characteristics at COSMO are also described by Inagaki & Kanda (2008). In general, the mean flow statistics are horizontally homogeneous, independent of the individual roughness cubes, at a height of 2H. The Reynolds stress is nearly constant,

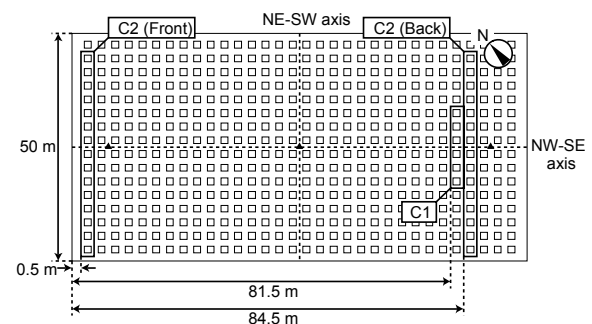


Figure 1 Schematic of experimental settings in COSMO: 10 Sonic anemometers were aligned in C1, and 15 sonic anemometers were aligned in C2(back).

and the mean velocity changes logarithmically in the vertical direction around 2H. Therefore, a measurement of the horizontal distribution of the turbulence was conducted at 2H where the logarithmic region develops.

3.2 Experimental settings

The sonic anemometers were aligned horizontally at 2H, and the velocity and temperature fluctuations were measured at each location in sync. This alignment is because of the measurement of the horizontal distribution of turbulent structures and the use of the spatial filtering. When the horizontal mean wind crosses this line, we obtained a horizontal-2D distribution of the velocity and temperature fluctuations by assuming Taylor's frozen turbulence hypothesis in the streamwise direction, and by direct measurement along the row of instruments. Based on this strategy, we used the following two instrument configurations.

In configuration 'C1', the 10 sets of Kaijo DA600 (TR-90AH) anemometers were aligned horizontally and parallel to the NE-SW axis at a constant height of 3.0 m from the ground as indicated in Figure 1. The probe heads of the anemometers were directed northwest because this study addresses only flow coming from this direction. The measurement points were spaced at a uniform 1.5-m distance. Therefore, the horizontal distribution of the measurement points ranges up to 13.5 m in the spanwise direction. The datasets were collected in sync at 50 Hz.

In the second configuration, 'C2', we used Young Model 81000 anemometers. Two sets of 15 Model 81000 devices were placed in 42-m straight lines along the NE-SW axis at the upwind and downwind sides of COSMO, as shown in Figure 1. The instruments were spaced at uniform 3-m intervals. The upwind and downwind rows were 84 m apart. All measured parameters, i.e., 30 sets of 3D velocity and temperature data, were collected in sync at a sampling rate of 10 Hz using a Chino KE3000 data logger. We only used the datasets obtained at the downwind law in this report.

4. RESULTS

4.1 Spectral characteristics of active turbulence

Figure 2 shows the ensemble averages of the turbulent velocity spectra of u , w and cospectra of uw derived from TD and SD using different sizes of filter size Δ . The frequencies were converted to wavenumbers by multiplying z'/U . The spectral densities were normalized by friction velocity u_* which is estimated from the root mean of $-uw$ at 2H. We confirmed that the shapes of the spectra of TD are well consistent with those of Kaimal et al. (1972) except the low frequency parts of u spectra (not shown).

The spectral energy of u at the lower frequencies was effectively reduced by the spatial filtering, although they are still not zero. With increasing the area for moving average Δ , the shapes of spectra of

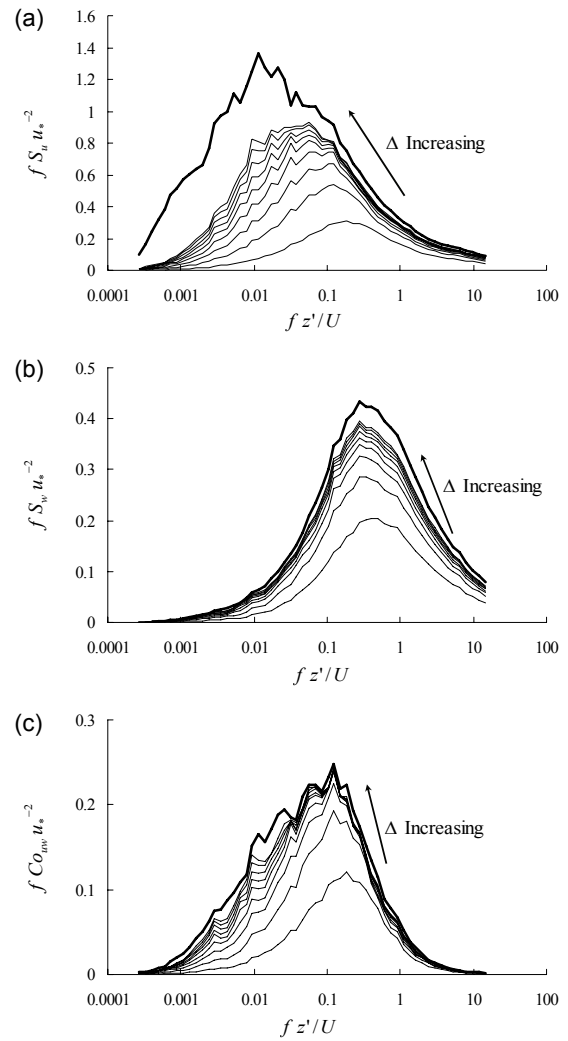


Figure 2 Turbulent spectra and cospectra of TD and SD fluctuations: (a) u , (b) w (c) uw . Bold line is non-filtered (TD) spectra, and thin lines are filtered (SD) spectra with different filter sizes Δ .

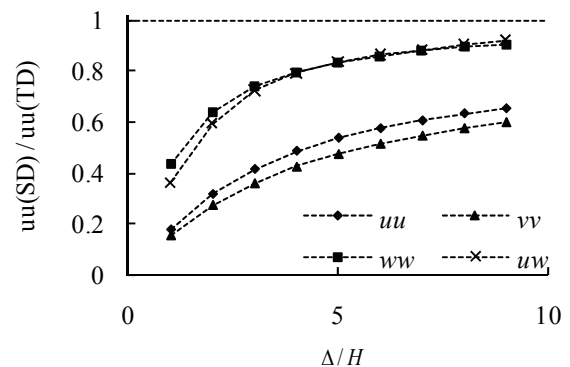


Figure 3 Relative contribution of the turbulent intensity of SD on that of TD for different filter size Δ .

SD reduce to those of TD. When the size of Δ is 9H,

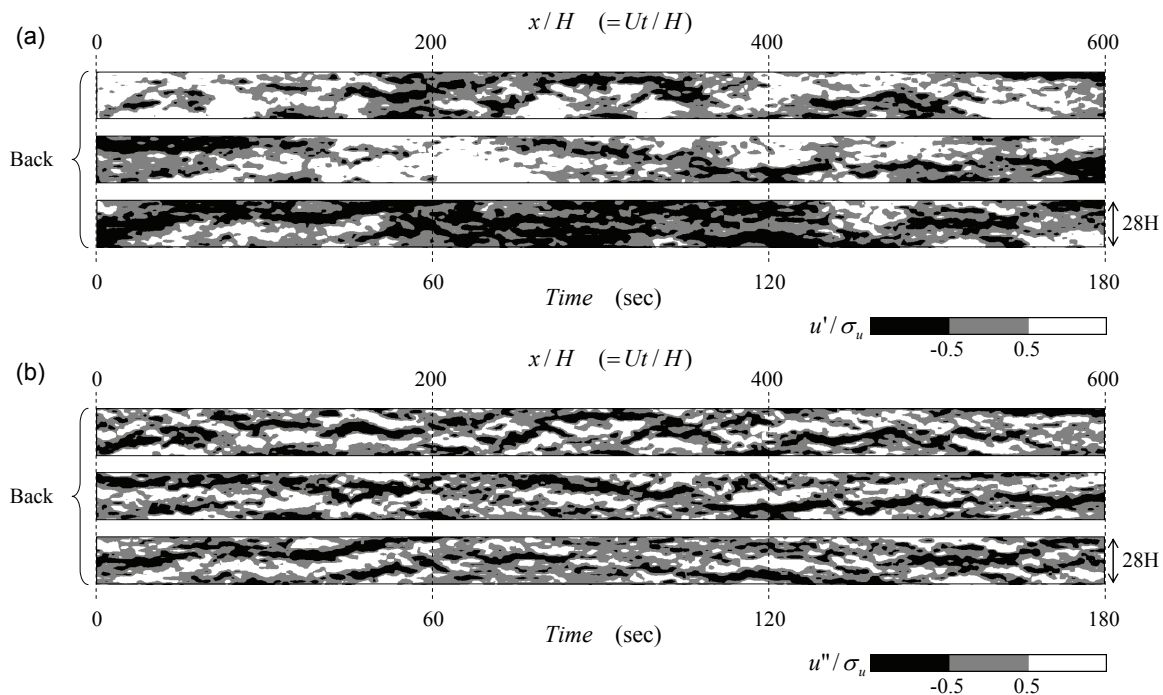


Figure 4 Horizontal distributions of u fluctuation: (a) non-filtered (TD), (b) filtered (SD). Black area indicates the negative fluctuation and white area indicates the positive fluctuation.

the entire shape of the w spectra and uw cospectra of SD are almost consistent with those of TD. However, the spectral shapes of u of SD at the lower frequency range still have considerable deficit from the TD spectra. This means that the low frequency motion of u , which is estimated from the spatial average along the spanwise direction, was nearly 'inactive' to the Reynolds stress. Meanwhile, the extracted fluctuation of SD represents the active motion.

Figure 3 shows the relative contribution of the turbulent intensity of SD on that of TD for different Δ . With increasing Δ , the relative contribution of uw of SD reduce to unity, which is about 0.95 when $\Delta/H = 9$. However, that of u is still much lower than uw . This deficit of the turbulent intensity of u is attributed to the contribution of the inactive motion which is separated by filtering.

4.2 Structural characteristics of active turbulence

A single 30-min dataset for the C2 configuration was extracted to visualize the horizontal distribution of u over the entire COSMO domain. In this period, the horizontal mean velocity was 5.0 m s^{-1} from the northwest at the measurement level, and the deviation of the mean wind direction was less than 1° from the NW-SE street axis. The flow is near-neutrally stratified ($\gamma = -0.0015$).

Figure 3 shows the horizontal distribution of u of TD and SD observed at the downwind side of COSMO ('C2 (Back)' in Figure 1). The size of the visualized field extends 9 min in time, which is comparable to about 2700 m (1800H) in the streamwise direction if we assume the frozen turbulence hypothesis, and 42 m (14H) in the spanwise direction. The figures were

folded every 3 min to keep the aspect ratio and to facilitate visualization.

The figure of the u -distribution of TD included a very large scale motion extended about a few minutes in the streamwise direction and covered the entire spanwise domain of COSMO.

In contrast, such low-frequency motions disappeared in the distribution of SD. Instead, streaky structures of low momentum region clearly appeared. This type of structure has been observed in the logarithmic layers during various field and numerical experiments, e.g., Hutchins & Marusic (2007) for flat filed in atmosphere experiments, Kanda et al. (2006) for cubic arrays in numerical simulations. Therefore, this is expected to be a universal characteristic of surface-layer turbulence regardless of the types of roughness.

Considering both the structural and spectral characteristics of TD and SD fluctuations of u , the very large structure of the elongated low momentum region is expected to be a part of the active motion. The inactive motion within the atmospheric surface layer is attributed to the motion included in the mixed layer, which is passing over the surface layer and propagates to the horizontal velocity fluctuation within the surface layer but not to the vertical velocity fluctuation.

4.3 Statistical characteristics of active turbulence

Inagaki and Kanda (2008) proposed a formula of the non-dimensional standard deviation of horizontal velocity fluctuation based on the inner-layer similarity with considering the contribution of the inactive fluctuation. The functional form is described as,

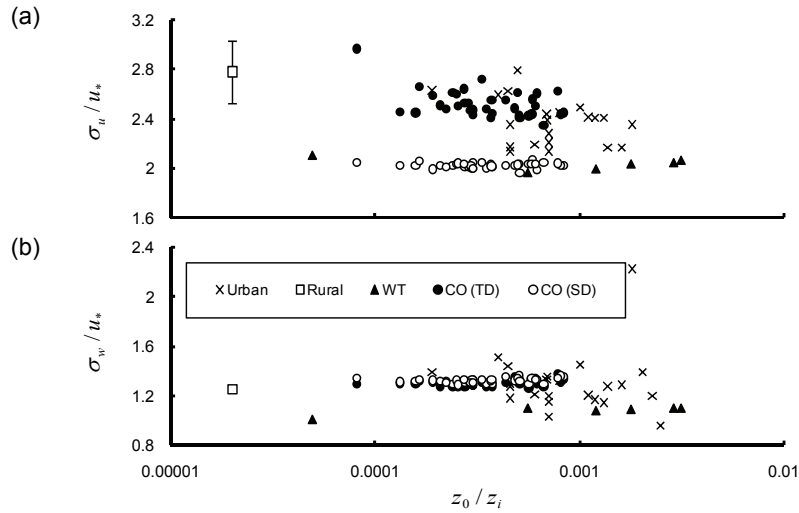


Figure 5 Non-dimensional standard deviations of (a) u and (b) w plotted for z_0/z_i : Urban (Roth 2000), Rural (Högström 1990), WT (wind tunnel, Raupach et al. 1991), CO (COSMO).

$$\left(\frac{\sigma_u}{u_*}\right)^2 = \alpha + \frac{u_{out}^2}{u_*^2}, \quad (3)$$

where, u_{out} is the contribution of inactive motion. The second term in the right hand side of eq.(3) represents the relative contribution of inactive and active fluctuation. Inagaki and Kanda (2008) guessed that this term is relevant to the ratio of the atmospheric boundary layer height z_i and roughness length z_0 .

Figure 5 shows the non-dimensional standard deviation of u and w observed in various experiments plotted on z_0/z_i . The values of u in TD depends on z_0/z_i as follows eq.(3). The values of w in TD is constant since inactive motion is just contribute to the horizontal velocity components. However, the values of u also reduced to a constant irrespective of z_0/z_i for the case of SD since the contribution of inactive motion is filtered out. This result implies that the horizontal velocity fluctuation can be explained by the inner-layer similarity in respect to the active motion.

5. CONCLUSIONS

The structural and statistical characteristics of active turbulence were investigated within the inertial sublayer over cubical roughness under atmospheric condition. The method to separate the active and inactive motion resulted in a reduced major part of the horizontal velocity spectra at low frequency region by subtracting the line averaged components, while preserving the entire Reynolds stress cospectra.

The horizontal distribution of the active motion included the very large scale motion of the elongated low momentum region, as found in various wind tunnel and atmospheric field experiments, and numerical simulations. Therefore, this structure is expected to be a universal characteristic of active motion in turbulent boundary layers. It is also shown that the active motion follows the inner-layer similarity irrespective of the inactive motion.

ACKNOWLEDGEMENTS

This research was partially supported by CREST (Core Research for Evolution Science and Technology) of JST (Japan Science and Technology cooperation), and the Ministry of Education, Science, Sports and Culture, Grant-in-Aid for Young Scientist (B): 21760382.

REFERENCES

- Hutchins, N., Marusic, I. 2007: Evidence of very long meandering features in the logarithmic region of turbulent boundary layers, *J. Fluid Mech.*, 579, 1-28.
- Högström, U. 1990 Analysis of turbulence structure in the surface layer with a modified similarity formulation for near neutral conditions. *J. Atmos. Sci.* 47, 1949–1972.
- Inagaki, A., Kanda, M., 2008: Turbulent flow similarity over an array of cubes in near-neutrally stratified atmospheric turbulence, *J. Fluid Mech.*, 615, 101-120.
- Inagaki, A. and Kanda, M., 2010: Organized structure of active turbulence developed over an array of cube within the logarithmic layer of atmospheric flow, *Boundary-Layer Meteorol.*, **135**, 209-228.
- Kanda, M., Kanega, M., Kawai, T., Sugawara, H., Moriwaki, R. 2007: Roughness lengths for momentum and heat derived from outdoor urban scale models, *J. App. Meteorol. and Climatol.*, 46, 1067–1079.
- Raupach, M. R., Antonia, R. A., Rajagopalan, S. 1991: Rough-wall turbulent boundary layers. *Appl. Mech. Rev.* 44, 1–25.
- Roth, M. 2000: Review of atmospheric turbulence over cities. *Q. J. Roy. Meteorol. Soc.* **126**, 941–990.
- Townsend, A. A. 1976: The Structure of Turbulent Shear Flow. *Cambridge University Press*.